Considerations on Fringing Fields of Quadrupole Lenses

By *Masahiro Ueda*, *Matu-Tarow Noda*

Department of Electronic Engineering, Ehime University, Matsuyama, Ehime, Japan

Koichi Nagami, and *Haruo Kuroda*

Department of Electronic Engineering, University of Osaka Prefecture, Sakai, Osaka, Japan

Abstract

The fringing potential distributions of electrostatic quadrupole lenses are investigated in great detail. The lenses are quadrupole singlet and doublet consisting of circular-concave electrodes with the gap between each electrode, 2γ $(= \pi/3)$. The distributions are calculated numerically in cylindrical coordinate (R, Θ, Z).

It is found that the rectangular hyperbolic equipotential is formed in the useful aperture region, the Θ-component and γ have negligible influences on the distributions, the R-component only has small influence on them, and the effective lens length hardly changes.

Inhalt

Überlegungen zu den Randfeldern von Quadrupollinsen. Die über die Linsenelektroden hinaustretenden Felder von elektrostatischen Quadrupollinsen werden untersucht. Betrachtet werden Singulett- und Dublett-Linsen mit kreis-konkaven Elektroden im Abstand $2\gamma = \pi/3$. Die Feldverteilung wird als Funktion der Zylinderkoordinaten R, Θ, Z numerisch berechnet. Es zeigt sich, daß die wirksame Potentialverteilung sich im entscheidenden Aperturbereich ausbildet. Die Θ-Komponente und γ haben einen vernachlässigbaren Einfluß. Die R-Komponente hat geringen Einfluß, und die effektive Linsenlänge ändert sich kaum.

1. Introduction

Since the quadrupole lens has been invented as a strong focusing lens for high-energy particle beams [1], many papers [2–5] have been published concerning its characteristics and applications. The lens systems have found many applications such as transportation of high-energy beams, stigmatic image formation like ordinary round lenses [6, 7], and special use utilizing their astigmatic characteristics [8–11]. Each lens system usually consists of a sequence of two or more lenses, since it is necessary to combine at least two quadrupole singlet lenses in series for a point focusing [12, 13].

To design the lens system precisely it is most important to know potential distributions along the beam axis, especially for strong and short lenses (in which the charged particle trajectories are strongly inclined with respect to the beam axis and the relative importance of the leakage fields is very much increased), but unfortunately it is rather difficult to measure them precisely in both magnetic and electrostatic lenses. In only a magnetic lens, they have been measured [14, 15].

In this paper the potential distributions for the electrostatic quadrupole lenses are analyzed by solving the three-dimensional Laplace equation numerically and they are compared with the ones obtained by experiments. The lens systems considered here are quadrupole singlet and doublet consisting of circular-concave electrodes for both a simplicity of mechanical realization and a convenience of analysis, but the results obtained here would be applicable to such other types of electrodes as plane, semi-cylindrical and hyperbolic electrodes.

2. Boundary Conditions for Computations

Since the magnetic and electric fields do not terminate in the beam direction abruptly at the ends of the quadrupole lens electrodes, there exist leakage fields called fringing fields which extend beyond the lens electrodes. For the analysis of this fields it is required to know potential distributions at the boundaries which enclose the entire lens region where the fields can not be neglected. These potential distributions may be taken as boundary conditions for the three-dimensional Laplace equation and are studied in this chapter.

Cylindrical coordinate (R, Θ, Z) are used for the convenience of the analysis.

2.1 *Lens Systems*

The configuration of the quadrupole singlet is shown in Fig. 1. The lens consists of portions of circles arranged on the cylindrical surface of radius a and separated by the gap 2γ, and it has the mechanical length 2 l_1 in the direction of the beam axis, i.e. Z-axis. The plane normal to Z-axis at $Z = 0$ is

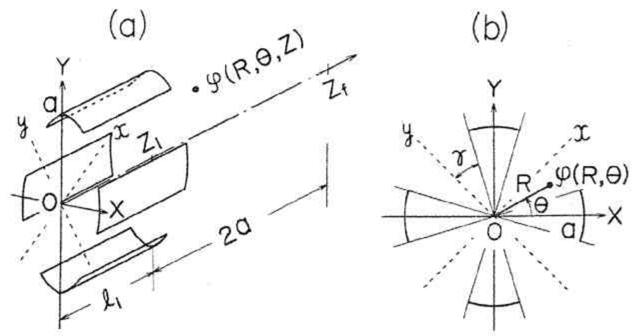

Fig. 1. Arrangement of the electrostatic quadrupole singlet consisting of circular-concave electrodes. (a) Construction of the system. (b) Cross-section of the lens.

then the symmetrical plane perpendicular to the axis. As discussed later, the gap between each electrode is chosen in such a way that the equipotentials within the useful aperture region are in satisfactory agreement with the rectangular hyperbolae, i.e. ideal potential distributions, with the axes Ox and Oy as asymptotes.

The quadrupole doublet composed of a sequence of the two quadrupole singlets is shown in Fig. 2. The planes normal to Z-axis at $Z = 0$ and $Z = Z_s$ are also the symmetrical planes through the axis as in the case of the quadrupole singlet.

2.2 *Potential Distributions in the Aperture Planes*

In the analysis of this distributions, $\varphi(R, \Theta)$, it is necessary to know potential distribution at the boundary, i.e. at the surface $R = a$, $\varphi(a, \Theta)$. The potential distribution is assumed as shown in Fig. 2(b). Then the potential distribution in the aperture plane, $\varphi(R, \Theta)$, is known as a solution of boundary value problem of the two-dimensional Laplace equation and is expressed as follows [16],

$$\varphi(R,\Theta) = \frac{4 V_0}{\pi} \sum_{m=0}^{\infty} \left\{ \frac{(-1)^m}{2m+1} \cdot \frac{\sin 2(2m+1)\gamma}{2(2m+1)} \cdot (R/a)^{2(2m+1)} \cdot \cos 2(2m+1)\Theta \right\}. \quad m = 0, 1, 2, \cdots \tag{1}$$

It can be seen from (1) that, if $R/a \ll 1$, the fundamental term corresponding to $m = 0$ dominates the behavior of $\varphi(R, \Theta)$ and then the rectangular hyperbolic equipotential distribution, i.e. quadrupole field, is formed. If there is complete symmetry of geometry, the first additional component which corresponds to $m = 1$ will be of 12-pole form. These facts are valid for other types of electrodes such as plane and semi-cylindrical electrodes [14, 17]. It is found that, if the gap 2γ is chosen to be $\pi/3$, the amplitude of this 12-pole component vanishes. More detailed discussions are treated in [16].

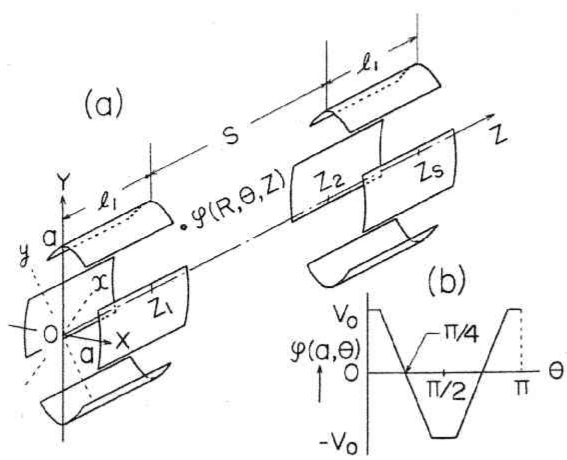

Fig. 2. Arrangement of the quadrupole doublet. (a) Construction of the lens system. (b) Potential distribution at the surface $R = a$ in the region $0 \leq Z \leq Z_1$.

Since, in the case of $l_1 \gg a$, end effects hardly appear near the center, $Z = 0$, of the lens [14], the potential distribution in (1) can be taken as one of the boundary conditions for the calculations of $\varphi(R, \Theta, Z)$ as follows.

$$\varphi(R, \Theta, 0) \simeq \varphi(R, \Theta). \tag{2}$$

In the neighborhood of the end of the electrode the potential becomes functions of three variables; R, Θ and Z. Since the normalized potential, $\varphi(R, \Theta, Z)/\varphi(R, \Theta, 0)$, is almost independent of Θ-variable for each value of R as seen in reference [14], $\varphi(R, \Theta, Z)$ can be assumed to be

$$\varphi(R, \Theta, Z) = f(Z) \cdot \varphi(R, \Theta, 0). \tag{3}$$

The function f(Z) is called the characteristic function of the lens. It is a rapid decreasing function of $|Z|$ for $|Z| > l_1$ and approaches to a few percent of f(0) at $|Z_f| = l_1 + 2a$. Therefore it can be reasonably assumed that the potential, $\varphi(R, \Theta, Z)$, is zero outside that region. Then another potential distribution for the boundary conditions is given by

$$\varphi(R, \Theta, Z_f) = f(Z_f) \cdot \varphi(R, \Theta, 0). \tag{4}$$

In the case of quadrupole doublet, the potential distribution at the center, $Z = Z_2$, of the second quadrupole singlet is determined by

$$\varphi(R, \Theta, Z_2) = c \cdot \varphi(R, \Theta, 0), \tag{5}$$

where c is a ratio of potentials of the second quadrupole electrodes to the ones of the first electrodes in the X-Z(or Y-Z) plane.

2.3 *Potential Distributions at the Surface $R = a$*

Besides the potential distributions mentioned above the other distributions in the surface at $R = a$ are required for the analysis of $\varphi(R, \Theta, Z)$ in both quadrupole singlet and doublet.

2.3.1 The Case of Quadrupole Singlet

The potential distributions at the surface $R = a$ are composed of two kinds of distributions. One is taken in the region $0 \leqq Z \leqq Z_1$ and is shown in Fig. 2(b). The other is taken in the region $Z_1 \leqq Z \leqq Z_f$ and is assumed to be given by

$$\varphi(a, \Theta, Z_1 \leqq Z \leqq Z_f) = \varphi(a, \Theta, 0 \leqq Z \leqq Z_1)/\exp\{(Z - l_1)/b\}, \tag{6}$$

where b is a parameter to be determined experimentally.

2.3.2 The Case of Doublet

In this case the potential distributions are composed of three kinds of distributions. The first distribution corresponds to the region $0 \leqq Z \leqq Z_1$ and is given in Fig. 2(b). The second one corresponding to the region $Z_2 \leqq Z \leqq Z_S$ is given by

$$\varphi(a, \Theta, Z_2 \leqq Z \leqq Z_S) = c \cdot \varphi(a, \Theta, 0 \leqq Z \leqq Z_1). \tag{7}$$

The last one is taken in the region $Z_1 \leqq Z \leqq Z_2$. It could be seen from the results by *H. Kawakatsu* et al. [15] that the measured fringing potential distributions of the lens are equal to a good approximation to the sum of the distributions of the individual quadrupole singlet. Therefore the potential distribution in that region can be reasonably assumed as follows

$$\varphi(a, \Theta, Z_1 \leqq Z \leqq Z_2) = \left(\frac{S + l_1 - Z}{S}\right)^n \cdot \varphi(a, \Theta, 0 \leqq Z \leqq Z_1)/\exp\{(Z - l_1)/b\}$$

$$+ \left(\frac{Z - l_1}{S}\right)^n \cdot \varphi(a, \Theta, Z_2 \leqq Z \leqq Z_s)/\exp\{-(Z - l_1 - S)/b\}, \qquad (8)$$

where n is also the parameter to be determined experimentally. The first term of the right hand side in (8) means a contribution to the potential at the boundary by the lens centered at $Z = 0$ and the second one by the lens centered at $Z = Z_S$. If $n = 0$, the first term becomes (6).

2.3.3 Determination of b and n

The two parameters, b and n, should be chosen in such a way that the calculated distributions with these parameters fit in satisfactory agreement with the experimental results.

Figure 3 shows the characteristic function f(Z) for some values of b with the experimental one obtained from electrolytic tank method by dots [18]. It can be seen from the figure that the appropriate values of b is 0.48a.

The two factors in (8), $\{(S + l_1 - Z)/S\}^n$ and $\{(Z - l_1)/S\}^n$, are introduced mainly to bring the analytic potentials into agreement with the ones on each electrode at $Z = Z_1$ and Z_2. Since the fringing potential distribution of the doublet is given approximately by the superposition of the ones of each singlet as mentioned above, the value of n should be small enough compared with 1. Figure 4 shows the analytic potential distribution expressed in (8) with $n = 0.125$ and the experimental results [18]. It is then ieasonable to choose $n = 0.125$.

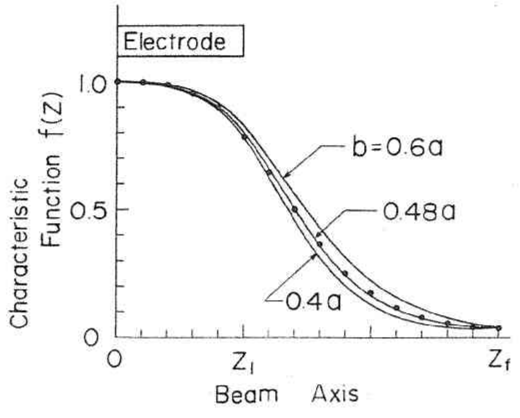

Fig. 3. Characteristic function f (Z) in the quadrupole singlet of $a = l_1$ and $\gamma = \pi/6$ for some values of b on the line of $R/a = 0.2$ and $\Theta = 0°$ with $f(Z_f) = 0.04$. Dots show the experimental results.

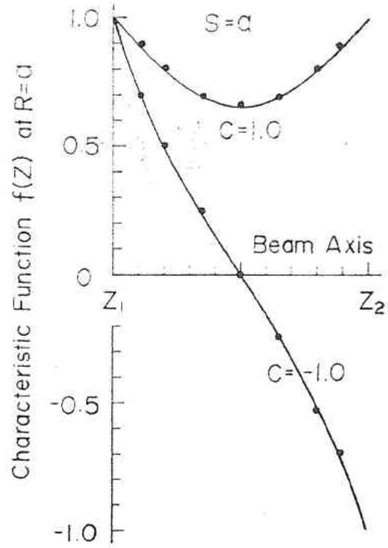

Fig. 4. Normalized potential distribution at the surface R = a in the region $Z_1 \leqq Z \leqq Z_2$ calculated from (8) with b = 0.48a, n = 0.125 and c = ± 1.0. Dots show the experimental results.

3. Results and Considerations

Numerical calculations are done by means of Liebmann's accelerating method in steps of 0.1a, $\pi/24$ and 0.1a for R-, Θ- and Z-coordinates, respectively.

3.1 *Potential Distributions in the Aperture Plane*

Table 1 shows the normalized potential distribution, $\varphi(R, \Theta)/V_0$, obtained by solving the two-dimensional Laplace equation numerically and the ideal

Table 1
Normalized potential distribution, φ (R, Θ)/ V_0, in the aperture plane for some combinations of the values of R/a and Θ with the lens of $\gamma = \pi/6$.

Results obtained by solving two-dimensional Laplace's equation numerically					
θ \ R/a	0.1	0.2	0.3	0.5	0.7
0°	0.0107	0.0428	0.0958	0.2657	0.5176
15°	0.0093	0.0370	0.0831	0.2303	0.4525
37.5°	0.0028	0.0111	0.0248	0.0687	0.1331
Results calculated from (1) with m=0 (ideal potential distribution)					
0°	0.0105	0.0421	0.0948	0.2632	0.5159
15°	0.0091	0.0365	0.0821	0.2280	0.4468
37.5°	0.0027	0.0109	0.0245	0.0681	0.1335

one calculated from (1) with $m = 0$ for some values of R/a and Θ. It is seen that the ideal potential distribution can be realized with a reasonable accuracy.

It has also been seen that the potentials obtained numerically agree quite well with the ones calculated from (1) if the higher order terms are considered.

3.2 *R- and Θ-Dependences of the Characteristic Function*

Figure 5 shows the characteristic function f(Z) for some values of R/a in the plane of $\Theta = 0°$ with the quadrupole singlet. It shows that the R-component has only small effect on f(Z) in the useful aperture region ($R/a \leqq 0.5$) and then an effective lens length L_{eff} which is defined by

$$L_{eff} = \frac{1}{f(0)} \cdot \int_{-\infty}^{\infty} f(Z)\, dZ \simeq \frac{2}{f(0)} \cdot \int_{0}^{Z_f} f(Z)\, dZ \tag{9}$$

hardly changes irrespective of the value of R/a. It also shows that $f(Z) \simeq 1$ in the region $|Z| \leqq Z_1 - a$. Therefore if $l_1 \geqq a$ the potential distribution expressed in (1) can be reasonably adopted as one of the boundary conditions for the three-dimensional Laplace equation.

Table 2 shows the characteristic function for some combinations of the values of R/a, Θ and Z with the same lens structure mentioned above. It is found that Θ-component has negligible influence on the characteristic function for various values of R/a and Z.

From the above discussions that R- and Θ-components have only small effects on the characteristic function, it is seen that almost perfect rectangular hyperbolic potential distribution is formed in any plane normal to Z-axis in the useful aperture region.

3.3 γ-Dependence of the Characteristic Function

As discussed in section 2.2 the gap between each electrode 2γ is chosen to be $\pi/3$ in order to minimize the second order term of the potential corre-

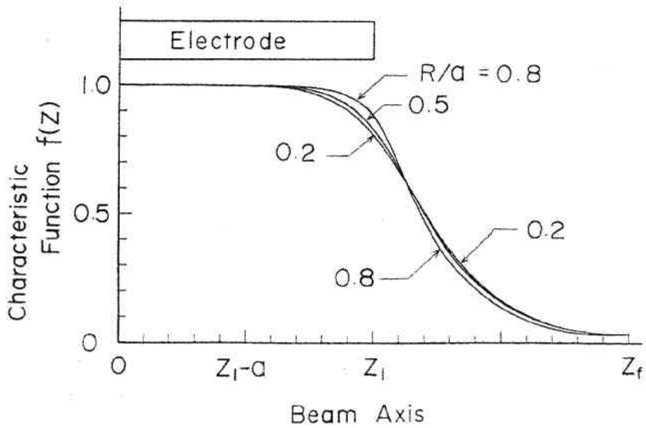

Fig. 5. Characteristic function f (Z) for some values of R/a in the quadrupole singlet of $l_1 = 2a$ and $\gamma = \pi/6$ with $b = 0.48a$ and $f(Z_f) = 0.04$ in the plane of $\Theta = 0°$.

Table 2

Characteristic function f (Z) in the quadrupole singlet of $l_1 = 2a$ and $\gamma = \pi/6$ for some combinations of the values of R/a, Θ and Z with b = 0.48a and f $(Z_f) = 0.04$.

R/a	Θ \ Z	$\ell_1/2$	$\ell_1 (=Z_1)$	$\ell_1 + a$
0.2	0°	0.997216	0.807516	0.172063
	15°	0.997209	0.807519	0.172053
	30°	0.997253	0.807548	0.172026
0.5	0°	0.998178	0.828946	0.161936
	15°	0.998167	0.829018	0.161913
	30°	0.998185	0.828947	0.161936
0.8	0°	0.999430	0.891108	0.142428
	15°	0.999439	0.892698	0.142075
	30°	0.999415	0.891111	0.142426

sponding to m = 1, and then all the results except for table 3 are obtained with this gap.

Table 3 shows the characteristic function for some values of γ. It shows that the gap has negligible influence on f(Z). From the insensitivity it may be suggested that the results obtained in this paper are applicable to other

Table 3

Characteristic function f (Z) in the quadrupole singlet of $l_1 = 2a$ for some values of γ with b = 0.48a and f $(Z_f) = 0.04$ on the line of R/a = 0.2 and $\Theta = 0°$.

Z \ γ	0°	15°	30°	45°
0	1.00000	1.00000	1.00000	1.00000
$0.2\ell_1$	0.99992	0.99983	0.99986	0.99986
$0.4\ell_1$	0.99890	0.99891	0.99894	0.99893
$0.6\ell_1$	0.99282	0.99284	0.99286	0.99287
$0.8\ell_1$	0.95742	0.95745	0.95750	0.95752
$\ell_1 (=Z_1)$	0.80741	0.80745	0.80752	0.80757
$\ell_1 + 0.4a$	0.50362	0.50362	0.50362	0.50360
$\ell_1 + 0.8a$	0.25246	0.25245	0.25244	0.25241
$\ell_1 + 1.2a$	0.11636	0.11635	0.11634	0.11633
$\ell_1 + 1.6a$	0.05673	0.05671	0.05671	0.05671
$\ell_1 + 2a (=Z_s)$	0.04000	0.04000	0.04000	0.04000

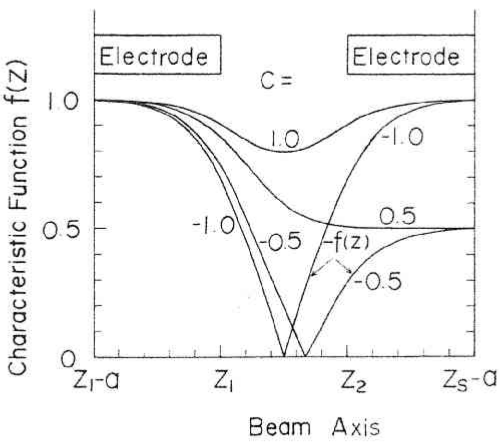

Fig. 6. Characteristic function f (Z) for some values of c in the quadrupole doublet of $l_1 = 2a$, $S = a$ and $\gamma = \pi/6$ with $b = 0.48a$ and $n = 0.125$ on the line of $R/a = 0.2$ and $\Theta = 0°$.

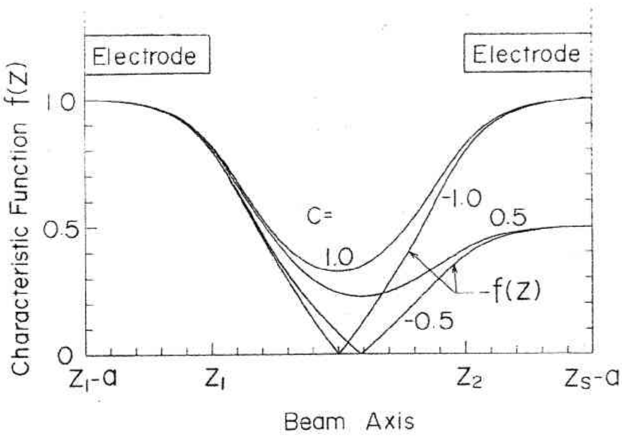

Fig. 7. Characteristic function for some values of c in the quadrupole doublet of $l_1 = 2a$, $S = 2a$ and $\gamma = \pi/6$ with $b = 0.48a$ and $n = 0.125$ on the line of $R/a = 0.2$ and $\Theta = 0°$.

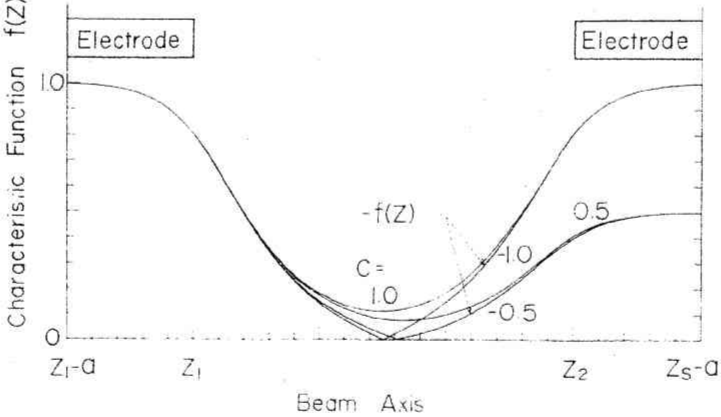

Fig. 8. Characteristic function for some values of c in the quadrupole doublet of $l_1 = 2a$, $S = 3a$ and $\gamma = \pi/6$ with $b = 0.48a$ and $n = 0.125$ on the line of $R/a = 0.2$ and $\Theta = 0°$.

types of electrodes such as plane, semi-cylindrical and hyperbolic electrodes. These facts have been verified experimentally [15, 17].

3.4 *Characteristic Function in the Quadrupole Doublet*

The results within the region $Z_1 - a \leqq Z \leqq Z_S - a$ are shown in Figs. 6, 7 and 8 for S = a, 2a and 3a, respectively. In each figure four cases corresponding to $c = \pm 1.0$ and $c = \pm 0.5$ are shown.

4. Conclusion

The fringing fields of electrostatic quadrupole lenses consisting of circular-concave electrodes have been analyzed numerically by using Liebmann's accelerating method. It was found that (1) the ideal potential distribution, i.e. rectangular hyperbolic equipotential, is formed in the useful aperture region if the gap is chosen properly,

(2) the Θ-component and γ have negligible effects on the fringing potential distributions along the beam axis, i.e. characteristic function,

(3) the R-component only has small effect on the characteristic function,

(4) the effective lens length hardly changes irrespective of R- and Θ-components and γ,

and finally

(5) these results obtained in this paper will be applicable to other types of electrodes such as plane electrode, cylindrical electrode and hyperbolic electrode.

Acknowledgment

M. Ueda and *M. T. Noda* would like to express their sincere thanks to Prof. *K. Ieyasu* and Dr. *T. Yamamoto* of Ehime University for their continuous interests and valuable discussions. Numerical calculations were done on FACOM 230–60 at the Data Processing Center of Kyoto University and FACOM 230–60 at the Computer Center of Kyushu University.

References

[1] *M. S. Livingston* and *J. P. Blewett*, Particle Accelerators, New York: McGraw-Hill, 1962, p. 112–117.
[2] *P. W. Hawkes*, Quadrupole Optics (Springer Tracts in Modern Physics, 42), Berlin, Heidelberg: Springer-Verlag, 1966.
[3] *J. J. Livingood*, Principle of Cyclic Particle Accelerators, Toronto: D. Van Nostland, 1971, p. 299–318.
[4] *A. P. Banford*, The Transport of Charged Particle Beams, London: E&F.N. Spon Limited, 1966, p. 92–120.
[5] *P. Grivet*, Electron Optics, Oxford: Pergamon Press, 1972, p. 287–322.
[6] *H. Kawakatsu*, J. Electron Microsc. *19* (1970) 121.
[7] *P. W. Hawkes*, Quadrupoles in Electron Lens Design (Advances in Electronics and Electron Physics. suppl. 7, *L. Marton* Ed.), New York: Academic Press, 1970.
[8] *C. F. Giese*, Rev. Sci. Instr. *30* (1959) 260.

[9] *S. Penner*, Rev. Sci. Instr. *32* (1961) 150.
[10] *H. Kawakatsu* and *K. Kanaya*, Bull. Electrotech. Lab. *33* (1969) 1279.
[11] *M. Ueda*, *K. Nagami* and *H. Kuroda*, Oyo-Buturi *38* (1969) 1037.
[12] *P. Junior* und *P. Antony-Spies*, Z. angew. Phys. *22* (1967) 420.
[13] *A. D. Dymnikov* and *S. Ya. Yavor*, Sov. Phys. Tech. Phys. *8* (1964) 639.
[14] *L. Marton*, Advances in Electronics and Electron Physics, New York and London: Academic Press, 1961, p. 86–203.
[15] *H. Kawakatsu*, *G. Vosburgh* and *B. M. Siegel*, J. Appl. Phys. *39* (1968) 245.
[16] *T. Hayashi* and *N. Sakudo*, Rev. Sci. Instr. *39* (1968) 958.
[17] *G. E. Lee-Whiting* and *L. Yamazaki*, Nucl. Instr. Meth. *94* (1971) 319.
[18] *M. Ueda*, *K. Nagami* and *H. Kuroda*, presented at the 17th Annu. Meeting Applied Physics in Japan, 1970, Lecture 2aG10.